Title
Stoichiometry and resource allocation in marine bacteria

Journal
Environmental Microbiology, 16(5)

ISSN
1462-2912

Authors
Zimmerman, Amy E
Allison, Steven D
Martiny, Adam C

Publication Date
2014-05-01

DOI
10.1111/1462-2920.12329

Peer reviewed

Phylogenetic constraints on elemental stoichiometry and resource allocation in heterotrophic marine bacteria

Amy E. Zimmerman[1,3]*, Steven D. Allison[1, 2], and Adam C. Martiny[1, 2]

[1]Department of Ecology and Evolutionary Biology and [2]Department of Earth System Science, University of California, Irvine, CA 92697 USA

[3]Monterey Bay Aquarium Research Institute, Moss Landing, CA 95039 USA

*Corresponding author

AE Zimmerman

Monterey Bay Aquarium Research Institute

7700 Sandholdt Road

Moss Landing, CA 95039-0628 USA

Phone: (+1) 831-775-1903

Fax: (+1) 831-775-1620

E-mail: amyz@mbari.org

Running title: Stoichiometry and resource allocation of marine bacteria

Keywords: element cycles and biogeochemical processes, microbial ecology, bacteria, resource allocation, growth and survival

SUMMARY

The objective of this study was to evaluate the contribution of evolutionary history to variation in the biomass stoichiometry and underlying biochemical allocation patterns of heterotrophic marine bacteria. We hypothesized that phylogeny significantly constrains biochemical allocation strategy and elemental composition among taxa of heterotrophic marine bacteria. Using a 'common garden' experimental design, we detected significant interspecific variation in stoichiometry, macromolecule allocation, and growth rate among 13 strains of marine Proteobacteria. However, this variation was not well explained by 16S rRNA phylogenetic relationships or differences in growth rate. Heterotrophic bacteria likely experience C-limitation when consuming resources in Redfield proportions, which consequently decouples growth rate from allocation to rRNA and biomass P content. Accordingly, overall bacterial C:nutrient ratios (C:P = 77, C:N = 4.9) were lower than Redfield proportions, whereas the average N:P ratio of 17 was consistent with the Redfield ratio. Our results suggest that strain-level diversity is an important driver of variation in the C:N:P ratios of heterotrophic bacterial biomass and that the potential importance of non-nucleic acid pools of P warrants further investigation. Continued work clarifying the range and controls on the stoichiometry of heterotrophic marine bacteria will help improve understanding and predictions of global ocean C, N, and P dynamics.

INTRODUCTION

Current models of ocean biogeochemistry assume that carbon (C), nitrogen (N), and phosphorus (P) cycle according to the "Redfield ratio" (molar C:N:P = 106:16:1) (Moore et al., 2004; Aumont and Bopp, 2006; Follows et al., 2007). This canonical ratio was derived from Alfred Redfield's observations of the stoichiometric similarity between dissolved nutrients in seawater and the biomass of marine plankton (Redfield, 1934). Subsequent studies investigating the biomass stoichiometry of marine plankton have detected variability across space and time, as well as between different species (e.g., Karl et al., 2001; Michaels et al., 2001; Quigg et al., 2003, 2011; Martiny et al., 2013a). Most of these studies have examined autotrophic phytoplankton, yet the contribution of heterotrophic bacteria to marine microbial biomass can occasionally surpass that of autotrophic phytoplankton (Ducklow, 1999; Pomeroy et al., 2007; Buitenhuis et al., 2012). Compared to autotrophs, the stoichiometry of heterotrophic bacteria remains poorly understood.

In marine systems, remineralization of organic C, N, and P is primarily driven by heterotrophic bacteria (Cotner and Biddanda, 2002; Kirchman, 2008), and is influenced by the stoichiometry of microbial biomass. For example, physiological regulation of biomass C:N:P composition relative to environmental supply determines whether marine bacteria are sources or sinks of mineral nutrients (Goldman et al., 1987; Tezuka, 1990). Bacterial stoichiometry also influences the trophic transfer of nutrients when bacteria are consumed (Güde, 1985; Martinussen and Thingstad, 1987; Shannon et al., 2007). Additionally, the elemental composition of bacterial biomass can impact the autotrophic component of the food web by affecting the nutrient that limits phytoplankton growth (Daufresne and Loreau, 2001; Danger et al., 2007).

Observed variation in C:N:P stoichiometry of marine plankton communities is likely due to a combination of physiological plasticity and phylogenetic constraints. For marine

phytoplankton, classical experiments demonstrated that nutrient supply ratio could drive biomass stoichiometry (Rhee, 1978). The flexibility in stoichiometric ratios (plasticity) is dependent on growth rate, with more constrained ratios at maximum growth rates (Klausmeier et al., 2008). Evolutionary history (phylogeny) imposes taxon-specific constraints on plasticity (Quigg et al., 2003, 2011), resulting from phylogenetically conserved differences among taxa in cellular architecture or ecological strategy. Accordingly, phytoplankton taxonomic composition can be a significant determinant of community biomass stoichiometry (Arrigo, 1999; Weber and Deutsch, 2010) and may be a significant contributor to global patterns in marine C:N:P (Martiny et al., 2013a).

Differences in stoichiometry due to physiological plasticity or phylogenetic conservation are likely linked to differences in biochemical allocation of cellular resources. Variation in cellular elemental composition is controlled by the differential partitioning of C, N, and P resources to various macromolecules according to ecological strategy (Klausmeier et al., 2004; Arrigo, 2005; Klausmeier et al., 2008). For example, the Growth Rate Hypothesis (GRH) predicts that greater allocation to P-rich ribosomes for growth will drive a cell to become enriched in P, reducing overall biomass C:P and N:P ratios (Elser et al., 1996; Sterner and Elser, 2002). However, evidence for the GRH has been derived largely from studies of zooplankton, phytoplankton, or *E. coli* (Elser et al., 2000, 2003). It remains unclear to what extent the GRH applies to marine heterotrophic bacteria, and subsequently, to what extent macromolecule allocation is linked to the biomass stoichiometry of marine bacteria.

Thus far, studies investigating the biomass stoichiometry of marine heterotrophic bacteria have been sparse and disparate (reviewed in Fagerbakke et al., 1996; Fukuda et al., 1998; Hochstädter, 2000). Evidence from several classical studies has shown that marine bacteria tend to be enriched in N and P relative to C with C:N:P ratios below Redfield (Bratbak, 1985; Goldman et al., 1987; Fagerbakke et al., 1996; Goldman and Dennett, 2000; Vrede et al., 2002), though substantial variation has been reported (Fukuda et al., 1998; Løvdal et al., 2008;

Chan et al., 2012). Furthermore, bacterial C:N ratios appear to be more constrained (Goldman et al., 1987; Goldman and Dennett, 2000), and C:P ratios more flexible (Bratbak, 1985; Cotner et al., 2010). These studies have demonstrated that similar to phytoplankton, the biomass stoichiometry of marine bacteria can vary in response to physical (e.g. temperature), chemical (e.g. resource ratio), and physiological parameters (e.g. growth phase), as well as among species. However, no study has yet reported on whether variation in elemental ratios and macromolecule allocation in marine heterotrophic bacteria is phylogenetically conserved.

Therefore, the objective of our study was to explicitly evaluate the contribution of phylogeny (evolutionary history) to variation in biomass stoichiometry and underlying biochemical allocation patterns in marine bacteria. We tested the hypothesis that phylogeny significantly constrains biochemical allocation strategy and elemental composition among taxa by cultivating diverse strains of marine bacteria under standardized conditions. This "common garden" approach was designed to minimize the effect of physiological plasticity and isolate inherent taxonomic differences in allocation and stoichiometry.

RESULTS

Using a common garden design with standardized resource and growth conditions, we evaluated the relationships among biomass stoichiometry, macromolecule allocation, growth, and phylogeny of 13 bacterial strains from two classes (Alpha and Gamma) within the Proteobacteria phylum, representing 7 prokaryotic families (Figure 1). The strains included a representative of the SAR11 cluster, Candidatus *Pelagibacter ubique* strain HTCC1062 (Rappé et al., 2002; Giovannoni et al., 2005), as well as three members of the marine Roseobacter group: *Oceanicola granulosus* HTCC2516, *Pelagibaca bermudensis* HTCC2601, and *Ruegeria pomeroyi* DSS-3 (Cho and Giovannoni, 2004, 2006; Moran et al., 2004). The remaining strains were isolated from coastal California seawater (see Supporting Information).

BIOMASS STOICHIOMETRY AND RELATION TO REDFIELD

Overall, marine bacteria tended to have low C:P and C:N ratios in relation to Redfield (molar C:N:P = 106:16:1) when supplied with carbon and nutrients in Redfield proportions. Strain-specific C:P ratio varied from 36 (HTCC1062) to 141 (DSS-3), with a geometric mean C:P ratio of 77 across all strains, significantly below the Redfield value of 106 ($p = 0.048$, Wilcoxon test, $n = 13$; Table 1). Nine strains had C:P ratios lower than Redfield (Figure 2a), though only five differences were statistically significant (HTCC2516, Alt1C, Vib1A, Hal146, Hal005; $p < 0.05$), and one was marginally significant (HTCC1062; $p = 0.06$). Mor119 did not differ significantly from Redfield C:P ($p = 0.88$), while DSS-3, HTCC2601, and Vib2D had C:P ratios that were greater ($p < 0.05$, except $p = 0.06$ for Vib2D). The C:N ratio was more consistent across strains than C:P (Figure 2c). The geometric mean ratio was significantly lower than Redfield (6.63) at 4.91 ($p = 0.001$, $n = 12$), and strain C:N ranged from 4.08 (Alt1C) to 7.35 (Vib2D). Nearly all strains had a C:N ratio below Redfield ($p < 0.05$, except $p = 0.06$ for Oce241, Oce340, Mor224, and Mor119), with the exceptions of DSS-3, which was not significantly different ($p = 0.81$) and Vib2D, which was greater ($p = 0.06$).

The geometric mean N:P molar ratio across all strains was 16.6, nearly equal to Redfield ($p = 0.42$, $n = 12$; Figure 2b; Table 1), with N:P ranging from 9.6 (Alt1C) to 25 (Mor119). However, no individual strain N:P ratio was equivalent to Redfield. Five strains (HTCC2516, Alt1C, Vib1A, Hal146, and Mor224) had an N:P ratio below 16 ($p < 0.05$, except $p = 0.06$ for Mor224), while the remaining 7 strains had N:P ratios greater than Redfield ($p < 0.05$, except $p = 0.06$ for Vib2D, Oce241, Oce340, and Mor119).

C:P ($K = 0.05$, $p = 0.42$), N:P ($K = 0.03$, $p = 0.86$), and C:N ($K = 0.16$, $p = 0.34$) ratios were weakly associated with phylogeny, as determined by phylogenetic signal analysis using Blomberg's K-statistic (Blomberg et al., 2003), which assumes a Brownian motion model of trait evolution. Non-parametric analysis of variance confirmed that C:P, N:P, and C:N ratios varied

148 significantly among the strains in our study ($p < 0.001$, Kruskal-Wallis ANOVAs); therefore, this
149 weak association was not due to lack of variation.
150
151 *GROWTH RATE AND ALLOCATION*
152 Similar to biomass stoichiometry, growth rate and biochemical allocation (whether
153 normalized to cell abundance or C biomass) were weakly associated with phylogeny, though
154 strains varied significantly in each trait ($p < 0.001$, Kruskal-Wallis ANOVAs). Growth rate varied
155 among strains from 0.009 to 0.621 hr^{-1} (HTCC1062 and Vib1A, respectively), with an overall
156 mean of 0.227 hr^{-1} (Figure 3; Table 1). Growth rate differences among strains did not show
157 significant phylogenetic signal ($K = 0.05$, $p = 0.69$), implying that evolutionary history was not a
158 strong predictor of measured growth rate for this group of organisms. Likewise, differences in
159 cellular C biomass (Table 1), a proxy for cell size, were not phylogenetically conserved ($K =$
160 0.06, $p = 0.65$), despite significant variation across strains ($p < 0.001$).
161 We also measured the concentration of DNA, RNA, and proteins. Average cell quota for
162 DNA among the strains was 3.1 fg $cell^{-1}$ (Figure S1a; Table 1), ranging from 0.65 (Mor119) to
163 6.7 fg $cell^{-1}$ (Oce340). RNA content was 4.8 times higher than DNA content on average. Cellular
164 RNA quota varied 100-fold among the strains, from 0.55 (Mor119) to 64.8 fg $cell^{-1}$ (Oce340),
165 with a grand mean of 17.7 fg $cell^{-1}$ (Figure S1b; Table 1). Average protein allocation was 76 fg
166 $cell^{-1}$ and was less variable across strains, ranging from 31 (HTCC2516) to 143 fg $cell^{-1}$ (Hal005;
167 Figure S1c; Table 1). No significant phylogenetic signal was detected for DNA ($K = 0.05$, $p =$
168 0.54), RNA ($K = 0.04$, $p = 0.68$), or protein ($K = 0.03$, $p = 0.79$) cell quotas.
169 When normalized to C biomass to account for potential variation in cell volumes among
170 the strains (e.g., Edwards et al., 2012) as well as possible inconsistencies between cell
171 concentrations determined by flow cytometry and the actual amount of cells retained on analysis
172 filters, DNA content was substantially less variable among strains, ranging from 0.004 (Mor119)
173 to 0.041 fg fg^{-1} C (Alt1C) with an overall mean of 0.022 fg fg^{-1} C (Figure 4a; Table S1). By

contrast, normalizing RNA and protein quotas to C biomass had little effect on variation across strains. RNA content ranged from 0.003 (Mor119) to 0.32 fg fg^{-1} C (Oce340), with an overall mean of 0.11 fg fg^{-1} C (Figure 4b; Table S1). Average allocation to protein across strains was 0.52 fg fg^{-1} C, and ranged from 0.25 (Mor119) to 0.81 fg fg^{-1} C (Alt1C; Figure 4c; Table S1). When normalized to C biomass, protein content showed significant phylogenetic signal (K = 0.60, p = 0.001), as did DNA content (K = 0.28, p = 0.01), though neither was strongly associated with phylogeny (e.g., K < 1). RNA content did not show significant phylogenetic signal (K = 0.05, p = 0.59).

The proportion of total cellular P resources bound in RNA (RNA-P) differed markedly among the strains in our study (p < 0.001, Kruskal-Wallis ANOVA, Figure 5). RNA-P represented a majority of cellular P content (>72%) for DSS-3, HTCC2601, Oce340, and Hal005, while RNA-P in the remaining strains represented 20% or less of the total P quota (Table 1). These differences did not depend on phylogenetic relationships among the strains (K = 0.09, p = 0.40).

LINKAGES BETWEEN GROWTH, ALLOCATION, AND STOICHIOMETRY

We used Spearman's rank correlations to determine associations among elemental composition, macromolecule content, and growth rate. DNA, RNA, and protein allocation, whether normalized to cell abundance or C biomass, were not significantly associated with elemental ratios (p > 0.05). Likewise, growth rate was not significantly related to C:P ratios, N:P ratios, or P content (normalized to C biomass, Figure 6a-c, or cell abundance, Figure S2a), as would be expected under the GRH. By contrast, growth rate was significantly and positively associated with RNA content (ρ = 0.587, p = 0.049 when normalized to C biomass, Figure 6d; ρ = 0.580, p = 0.052 when normalized to cell abundance, Figure S2b) across strains.

DISCUSSION

As a means of understanding potential drivers of variation in the elemental composition of marine heterotrophic bacteria, the objective of this study was to explicitly evaluate the contribution of evolutionary history (phylogeny) to measured variation among bacterial strains. The goal of our common garden approach was to minimize physiological plasticity in order to isolate taxonomic patterns in elemental stoichiometry, evaluate the linkages between stoichiometry and biochemical allocation strategy, and assess the phylogenetic conservation of these traits. We hypothesized that variation in the biomass stoichiometry of individual strains would be related to macromolecule allocation, and that both traits would follow phylogenetic relationships. Our results revealed significant strain-level variation in biomass stoichiometry and allocation strategy that was not strongly related to 16S ribosomal RNA phylogeny (i.e., long-term evolutionary history). Instead, resource allocation in marine heterotrophic bacteria likely varies at fine taxonomic resolution (i.e. on the scale of short-term evolutionary history). Consistent with previous observations of some heterotrophic bacteria (Neidhardt and Magasanik, 1960; Rosset et al., 1966; Kemp et al., 1993; Kerkhof and Ward, 1993; Poulsen et al., 1993; Wagner, 1994; Bremer and Dennis, 1996), overall RNA content increased with measured growth rate (Figures 6d, S2b). However, this relationship was not strong enough to significantly influence total biomass P content or C:P and N:P ratios as predicted by the Growth Rate Hypothesis (GRH), at least under the conditions of our study (Figure 6). Biomass stoichiometry and allocation to RNA may commonly be decoupled in heterotrophic marine bacteria if P is not the principal limiting resource and accumulates in biomass pools other than ribosomal RNA.

Overall, C:P and C:N biomass ratios of the strains in our study deviated from the Redfield ratios of C:P = 106 and C:N = 6.63, with a majority of the strains falling significantly below the Redfield value for both ratios (Figure 2a,c). Without knowing the minimum cell quotas

of C, N, and P for the strains in our study, we speculate that this pattern reflects general carbon limitation, which appears to be common for marine heterotrophic bacteria (Kirchman, 1990; Cherrier et al., 1996; Kirchman et al., 2000; Carlson et al., 2002). The average amount of biomass produced per mass of organic C consumed ("bacterial growth efficiency", BGE) has been estimated at 22% for heterotrophic marine bacteria (Del Giorgio and Cole, 1998), though there is substantial variation due to biotic and abiotic influences (Carlson et al., 2007). Assuming that all added organic C was consumed, BGE averaged 37% for the strains in our study and suggests generally high C-demand. Thus, C limitation and sub-Redfield C:P and C:N ratios may be prevalent among marine heterotrophs that consume resources with Redfield stoichiometry. By contrast, the average N:P ratio across strains was not statistically different from Redfield (Figure 2b).

The Growth Rate Hypothesis is one mechanism proposed for linking biomass stoichiometry and allocation strategy (Elser et al., 1996, 2000). However, tight coupling among growth rate, RNA content, and biomass P is primarily expected when P limits ribosome biogenesis and growth (Elser et al., 2003; Makino et al., 2003; Franklin et al., 2011). Widespread C limitation would imply that the GRH is probably a poor predictor of biomass stoichiometry among marine heterotrophic bacteria. Accordingly, we did not observe the predicted inverse relationship between growth rate and C:P or N:P ratio (Figure 6a,b) or the underlying positive relationship between biomass P and growth rate (Figure 6c, Figure S2a). The GRH assumes that rRNA is the primary pool of P biomass (Elser et al., 2003; Vrede et al., 2004), but total RNA was not a major determinant of biomass P for eight strains in our study (RNA-P = 11% of total P on average; Table 1). The other four strains (DSS-3, HTCC2601, Oce340, and Hal005) allocated a majority of their P resources to RNA (RNA-P = 87% of total P on average; Figure 5; Table 1) and may therefore have been growing at or near maximum growth rates. However, it is increasingly apparent that the relationship between growth rate and rRNA in bacteria is complex (Blazewicz et al., 2013).

Previous studies have indicated that the proportion of biomass P represented by RNA can vary substantially in other species of bacteria. In P-limited cultures of *Corynebacterium bovis*, Chen (1974) measured ~30% total cellular P bound as RNA. Makino et al. (2003) demonstrated that the allocation of P resources to RNA can vary in cultures of *E. coli* from 40-50% at lower growth rates up to 70-80% at higher growth rates. The magnitude of variation we measured in RNA-P among strains of marine bacteria is more similar to the variation reported for communities of lake bacteria (Makino and Cotner, 2004). In these communities, both growth (dilution) rate and substrate ratio influenced the contribution of RNA-P to total P, which varied from 25-43% under C-limitation to 76-93% under P-limitation. We recognize that there may be uncertainty in our RNA-P data because we did not account for potential differences in nucleic acid extraction efficiency among strains. Furthermore, the mass balance of intracellular resource pools is subject to technical limitations and influenced by uncertainty in the methods used to quantify various resource pools (e.g., Aschar-Sobbi et al., 2008). In spite of these potential limitations, our results suggest that pools of P other than nucleic acids, such as phospholipids or polyphosphate (Sterner and Elser, 2002; Makino et al., 2003; Makino and Cotner, 2004; Cotner et al., 2006), may be important in determining the C:P and N:P ratios of heterotrophic bacterial biomass. Similarly, non-nucleic acid P made up 3-70% of total biomass P in lake bacteria (Makino and Cotner, 2004), and polyphosphate production appears to be a widely distributed trait among heterotrophic bacteria (Harold, 1966; Kornberg et al., 1999). Unlike Cyanobacteria, heterotrophic marine bacteria probably cannot substitute phospholipids to reduce physiological P demand (Van Mooy et al., 2009).

We used our common garden experiment to explicitly evaluate the contribution of evolutionary history to variation in biomass stoichiometry, macromolecule allocation, and growth rate among marine bacteria. Traits were considered “phylogenetically conserved” when the values among related organisms were significantly more similar than expected by Brownian motion trait evolution (phylogenetic signal K-statistic > 1; Blomberg et al., 2003). Overall, 16S

rRNA phylogeny was not an important determinant of strain-level differences in elemental composition (Figure 2) or allocation to DNA, RNA, or protein content (Figure 4). We observed this result regardless of whether we analyzed elemental and macromolecule content per cell or normalized to C biomass. Furthermore, we did not detect significant phylogenetic signal in growth rate among the strains in our study (Figure 3), even though specific growth rate represents an integrated parameter of general life history strategy (Arendt, 1997). This lack of phylogenetic signal was not due to a lack of variation. Non-parametric analysis of variance confirmed that biomass stoichiometry, macromolecule allocation, and growth rate all varied significantly among the strains in our study ($p < 0.001$), indicating that within the Proteobacteria, there is substantial diversity at the strain level.

Our interpretation of phylogenetic signal is tempered by some limitations inherent in our approach, hence we do not imply that there can never be a relationship between phylogeny and growth rate (and possibly elemental ratios). The lack of phylogenetic signal in growth rate may be influenced by our selection of strains or the particular metric used to represent growth rate. For example, lineages like SAR11 may have an inherently different growth strategy compared to *Vibrio*, though it appears there may be substantial variation in growth rates within the SAR11 clade (Campbell et al., 2011). Expanding the phylogenetic breadth of the organisms in our analysis could increase the likelihood of detecting significant phylogenetic conservation in bacterial traits; however, distinct patterns supporting conservation of habitat preference and genome size, for example, have been demonstrated with less phylogenetic diversity than in our study (Ettema and Andersson, 2009). Likewise, our results may have differed if we were able to express growth rate relative to an empirically- or theoretically-determined maximum rate for each strain. Chrzanowski and Grover (2008) showed previously that relative growth rate, when measured as a percentage of maximum growth rate, explained a significant amount of the variance in the cellular C, N, and P quotas of *Pseudomonas fluorescens*.

Another consideration of our experimental approach is that C was provided as a mixture of defined sources in the growth media. The use of simple C substrates is highly variable among closely related strains of bacteria (Martiny et al., 2013b). Thus, it is probable that the organisms in our study could have differentially specialized on the various C sources provided, which has the potential to influence growth efficiency unequally across the strains. While this may have affected our results by generating additional variation in growth rate and stoichiometry, we consider potential differences in C resource use to be inherent characteristics of each strain, analogous to strain specific differences in cell quotas, and therefore valid contributions to our observed results. Furthermore, strain specific differences in C use are likely common in the ocean, where the combination of C compounds is variable and transient, influencing growth in numerous ways. Importantly, the strains in our study were supplied with the same resource combination under identical environmental conditions to meet our objective of evaluating the contribution of evolutionary history to variation in the stoichiometry and biochemical allocation patterns of marine bacteria.

Despite a weak phylogenetic signal, we observed significant strain-level variation in the biomass stoichiometry and allocation strategies of marine heterotrophic bacteria. This variation suggests that the genes controlling stoichiometric traits are evolving more rapidly than 16S rRNA. In bacteria, many traits related to resource use (Martiny et al., 2013b) or “adaptability processes” (Ettema and Andersson, 2009) are associated with specific taxa or ecotypes at ≥ 97% 16S rRNA gene sequence identity and are therefore difficult to resolve from traditional rRNA relationships. This pattern of fine-scale “microdiversity” (e.g., Martiny et al., 2006) may result from local adaptation or niche specialization, and likely reflects differential adaptation to environmental conditions among closely related organisms. Protein allocation appeared to be an exception and was generally consistent within families (Figure 4c), suggesting that constrained protein content in relation to C biomass may be a general pattern among marine bacteria (Simon and Azam, 1989; Kirchman, 2012). Overall, interspecific variation should be

329 considered when evaluating or predicting bacterial contributions to ecosystem processes. Such
330 variation may be especially important in low-diversity ecosystems that are dominated by few
331 bacterial species with substantially different elemental ratios.

332 In general, bacterial biomass P content is more variable than C or N content (Bratbak,
333 1985; Kirchman, 2000; Vrede et al., 2002; Cotner et al., 2010). This distinction may in part be
334 due to the similar N content in proteins and nucleic acids, such that organisms differing in
335 protein:nucleic acids ratios do not differ substantially in N content (Elser et al., 1996; Sterner
336 and Elser, 2002). Cellular protein contents measured in our study are comparable to previously
337 published values for other marine bacteria (Simon and Azam, 1989; Jeffrey et al., 1996; Zubkov
338 et al., 1999), but our values are lower than the cellular protein content measured for rapidly
339 growing *E. coli* (Bremer and Dennis, 1996; Kirchman, 2012). On average, C and N in nucleic
340 acids represented a small proportion of total N (7%), and even less of total C (4%) in our study.
341 The contribution of C and N bound in proteins to total cellular C and N quotas, by contrast,
342 represented more significant biomass pools of both elements, constituting 28% of total C and
343 37% of total N on average across strains. One of the limitations of our method is that it does not
344 account for the extraction efficiency of total protein; thus we may have underestimated the
345 proportion of cellular C and N bound in protein. However, cells contain other pools of cellular C
346 and N, including lipids, polysaccharides, and peptidoglycan (e.g., Vollmer et al., 2008). These
347 pools can contribute substantially to bacterial biomass (Sterner and Elser, 2002) and may
348 influence species-level differences in elemental composition.

349 We found that heterotrophic marine bacteria grown in the same resource environment
350 show significant strain-level differences in biomass stoichiometry, allocation strategy, and
351 growth rate. However, this diversity was not correlated with long-term evolutionary history, as
352 represented by 16S rRNA phylogenetic relationships. Our results suggest that the elemental
353 stoichiometry of marine plankton may depend on the taxonomic identity of heterotrophic
354 bacteria in the community. Our results also suggest that consumption of resources with near-

Redfield stoichiometry likely causes C limitation of marine heterotrophs and could result in C:nutrient ratios below Redfield. Low C:P and C:N biomass ratios indicate that heterotrophic bacteria may function as sinks of mineral nutrients (relative to C) in marine systems. This stoichiometric pattern may have consequences for material exported to the deep ocean, transfer of resources to higher trophic levels (Güde, 1985; Martinussen and Thingstad, 1987; Shannon et al., 2007), and limitation of algal growth (Daufresne and Loreau, 2001; Danger et al., 2007). These potential consequences warrant more explicit consideration of heterotrophic bacteria in ocean biogeochemical models. Additional empirical studies are also needed to characterize spatial and temporal variation in the abundance and stoichiometry of marine heterotrophic bacteria. Together, these efforts should improve predictions of broad patterns in global ocean biogeochemistry.

EXPERIMENTAL PROCEDURES

PHYLOGENETIC TREE CONSTRUCTION

16S rRNA gene sequences for strains HTCC1062, DSS-3, HTCC2516, and HTCC2601 were obtained from the Silva database (accession numbers CP000084, CP000031, AAOT01000021, and AATQ01000003, respectively; http://beta.arb-silva.de/; Pruesse et al., 2007; Quast et al., 2013), and aligned with the consensus sequences for all Newport Beach isolates using the SINA aligner (http://beta.arb-silva.de/aligner/; Pruesse et al., 2012). Three archaeal 16S rRNA gene sequence were included in the alignment as an outgroup (*Thermoproteus tenax*, GenBank accession no. M35966; *Sulfolobus solfataricus*, D26490; and *Methanococcus vannielii*, M36507). The phylogenetic tree topology was inferred from the multiple sequence alignment by maximum likelihood estimation with a search for the best tree, global rearrangements allowed, a transition/transversion ratio of 2.0, a constant rate of variation among sites, and nucleotide frequencies that were estimated from the data. Bootstrap

proportions were determined from 100 resamplings using the same maximum likelihood parameters. Phylogenetic tree construction was carried out with the PHYLIP software package (v3.69; Felsenstein, 2005). The FigTree program (v1.4.0; http://tree.bio.ed.ac.uk/software/figtree/) was used for visualization and to root the phylogeny at the midpoint to meet requirements for further phylogenetic analyses.

CULTURE CONDITIONS

All strains were revived on ½YTSS agar plates (González and Moran, 1997; Hardwick et al., 2003), and a single colony was picked to ensure purity prior to experiments. HTCC1062 was revived and grown only in liquid LNHM (Connon and Giovannoni, 2002) and monitored via flow cytometry (details below) for growth and contamination. Fresh cultures were used to initiate growth in a standard seawater media (SSM; Table S2) containing 87.5 μM sodium acetate, 29.17 μM D-glucose, 58.35 μM glycerol, 80 μM NH_4Cl, 5 μM K_2HPO_4, 1 nM L-methionine, 15 μM Na_2-EDTA, 95 μM Na_2CO_3, vitamins (10^{-4} dilution of stock; Rappé et al., 2002), and SN trace metals (10^{-3} dilution of stock; Table S6). Seawater used to prepare SSM for all growth experiments was collected from the San Pedro Ocean Time-Series Station (SPOTS; 33°33′00”N, 118°24′00”W) in January 2012, filtered (0.2-μm) and autoclave-sterilized, then diluted with high purity water (18.2 MΩ•cm) to 75% (by weight). SSM and culture conditions were designed to facilitate growth of a wide range of marine microorganisms (oligotrophs and copiotrophs), rather than to be optimal for any one organism, as well as to provide carbon (C), nitrogen (N), and phosphorus (P) resources in the molar Redfield ratio of ~106:16:1 (Redfield, 1958). Cultures were maintained in SSM in the dark at 20°C through several transfers to ensure proper growth prior to experiments. Growth profiles were established for each strain to determine the approximate time and culture concentration at the transition from log to stationary phase and were later used to guide sample collection. Cell abundance was estimated by flow cytometry (Marie et al., 2001) on an Accuri C6 flow cytometer (BD, Franklin Lakes, NJ, USA),

which was calibrated with beads once per week. Culture aliquots were fixed with glutaraldehyde (0.1% final concentration) and stained with SYBR Green-I nucleic acid dye (Molecular Probes, Inc., Eugene, OR, USA), then run in duplicate for one minute at a flow rate of 35 µL min^{-1}. Cytograms of green fluorescence versus side scatter were used to count and distinguish cells from media background. Cell abundances determined by flow cytometry were comparable to cell counts determined from dilution plating (unpublished data).

COMMON GARDEN EXPERIMENTS AND GROWTH RATE ANALYSIS

Replicate experimental cultures (n = 6) of each bacterial strain were grown in SSM with gentle mixing using the same 20°C incubator. Experimental cultures were initiated with $1.3x10^4$ (HTCC1062) to $1.3x10^5$ (Vib2D) cells mL^{-1} from 24-48 hour liquid cultures. Growth was monitored in near-real time with flow cytometry and samples were collected during late-log to early stationary phase when each culture reached approximately 75% maximum abundance. Culture concentrations were monitored after sample collection to confirm that collection occurred at the appropriate growth phase. All culture samples were collected onto pre-combusted (450°C, 5 hr) 0.3-µm-pore-size glass fiber filters (Sterlitech Corp., Kent, WA, USA) under gentle filtration. For nucleic acid and protein determinations, duplicate samples were collected from each culture replicate, flash frozen in liquid nitrogen, and stored at -80°C. Additional duplicate samples were collected from each culture replicate for evaluation of C/N (simultaneously) and P content, and stored at -20°C in acid washed and pre-combusted glass scintillation vials. Media blanks of sterile SSM were also collected as described.

All growth analyses were carried out in R using the “car” (Fox and Weisberg, 2011) and “stats” packages (R Core Team, 2012). Growth curves were established individually for each culture replicate by fitting a logistic growth model to the data: $y = \theta_1/(1 + \exp[-(\theta_2 + \theta_3 x)])$ (Fox and Weisberg, 2010), where the response, y, is the culture concentration, and the predictor, x, is hours. Initial parameters were estimated visually for the asymptote (θ_1), and using the self-

starting SSlogis function (Pinheiro and Bates) to estimate the value of x at the point of inflection (θ_2) and the scale parameter (θ_3). Maximum abundance was determined from the model and used to calculate growth rate as the exponential rate of change: μ (hr^{-1}) = $\ln(N_{75} - N_{25})/dt$, where N_{75} and N_{25} are the culture concentrations at 75% and 25% maximum abundance, respectively, and dt is the time interval (in hours) between observations. This method allowed us to target the most linear portion of each growth curve, and we excluded any individual replicates that showed unusual growth profiles. Additionally, we repeated all analyses with the subset of strains that were clearly collected during exponential growth (referred to as the "exponential only" dataset) to ensure that slight differences in growth phase were not significantly altering our results. This subset included HTCC1062, HTCC2516, HTCC2601, Alt1C, Vib2D, Oce241, Oce340, Mor224, and Mor119. Since all statistical results were similar with the full and exponential only datasets, we presented all strains in the main text, but included results from the exponential only subset in the Supporting Information (Tables S3, S4) for comparison of the two datasets.

ANALYTICAL METHODS: ELEMENTAL COMPOSITION

Biomass C and N content was determined using a CHN analyzer (Thermo Finnigan EA 1112, Bremen, Germany) after samples were treated with HCl (0.2M) to remove inorganic material and dried overnight at 65˚C. Sample C/N mass was calculated from chromatogram area using atropine standards and corrected for media blanks. P content was determined using an ash-hydrolysis method with $MgSO_4$ (0.017M) treatment previously described (Solorzano and Sharp, 1980; Lomas et al., 2010). Sample P was calculated from an asymptotic regression of absorbance vs. known concentrations of potassium phosphate standards (0-0.5 µmol) and corrected for media blanks. Atomic ratios were calculated for the C, N, and P content of samples, and the geometric means are reported for each strain. The amount of C, N, and P bound in specific macromolecules was calculated assuming nucleic acids are 33% C, 15% N, and 9% P, whereas protein is 53% C and 17% N on average (Sterner and Elser, 2002).

459

460 *ANALYTICAL METHODS: MACROMOLECULE CONTENT*

461 The quantification of DNA, RNA, and protein content was modeled after a previously
462 published method (Berdalet et al., 2005) and designed to avoid potential loss and degradation
463 resulting from the repeated isolation and cleaning steps of traditional extraction procedures.
464 High-sensitivity macromolecule-specific Quant-iT fluorophores (Molecular Probes, Inc., Eugene,
465 OR, USA) were used following a crude lysis to detect total DNA, RNA, and protein released
466 from cells. Dye selectivity and sensitivity as well as tolerance of contaminating substances are
467 available from the manufacturer. Standards, buffers, and reagents were stored and used
468 according to the manufacturer's suggestions.

469 Briefly, nucleic acids and proteins were released from filters by mechanical lysis (MP
470 FastPrep-24 bead beater, MP Biomedicals, Solon, OH, USA) in a solution of Tris buffer (5 mM)
471 and RNA preservative (saturated ammonium sulfate solution). Sample supernatant was used to
472 prepare assays in 96-well microplates with fluorescent dye, buffer, and pre-diluted standards
473 provided with each kit (*E. coli* rRNA, λ dsDNA, or BSA protein). Potential interference from cell
474 debris was tested using samples of *Roseovarius* sp. TM1035 collected as described above and
475 spiked with known amounts of each target macromolecule. Nearly 100% of added RNA and
476 DNA was detected (Figure S3a,b). Only the protein fluorophore showed significant interference
477 from cell debris (detected only 70 ± 5% added BSA protein; Figure S3c), so a spiked control of
478 strain Mor224 was included in each assay. Macromolecule concentrations were calculated
479 based on standard curve regressions of fluorescence vs. known standard concentrations. See
480 Supplemental Information for additional details.

481

482 *PHYLOGENETIC AND STATISTICAL ANALYSES*

483 Trait conservation was measured by phylogenetic signal using Blomberg's K-statistic
484 (Blomberg et al., 2003), which assumes a Brownian motion model of trait evolution where the

485 expected covariance between species' trait values is proportional to the shared evolutionary
486 history. K has an expected value of 1 when the traits have evolved by Brownian motion (e.g.,
487 descent with modification). K values < 1 indicate low phylogenetic dependence whereas K
488 values > 1 indicate that traits are more similar in related species than expected by Brownian
489 motion evolution. We considered K values > 1 as evidence of phylogenetic trait conservation.
490 Phylogenetic signal analyses were completed with the R package "picante" (Kembel et al.,
491 2010) using 999 randomizations for significance tests. We considered all statistical analyses to
492 be significant when $p < 0.05$.
493 We used a two-sided Wilcoxon signed rank test to test whether elemental ratios across
494 all strains (n = 12 or 13, depending on specific ratio) differed from Redfield proportions (C:P =
495 106, N:P = 16, or C:N = 6.63). We then used Wilcoxon tests to determine which individual
496 strains (n = 4-6 replicates) deviated significantly from Redfield stoichiometry. We tested for
497 significant strain-level variance in growth rate, elemental ratios, or macromolecule allocation
498 using Kruskal-Wallis ANOVAs with strain as a random factor. Linkages among elemental
499 composition, macromolecule content, and growth rate were quantified using Spearman's rank
500 correlations. Tests were implemented with the default "stats" package in R (R Core Team,
501 2012). Phylogenetic and statistical analyses of DNA, RNA, and protein allocation were done on
502 data normalized to cell abundance as well as C biomass.
503
504
505 **ACKNOWLEDGEMENTS**
506
507 We thank two anonymous reviewers for their insightful feedback, which greatly improved the
508 first versions of this manuscript. We thank Drs. Stephen Giovannoni and Mary Ann Moran for
509 supplying strains HTCC1062, DSS-3, HTCC2516, and HTCC2601 for the study. We also thank
510 Céline Mouginot for collecting seawater for the growth media, Dr. Jennifer Martiny for the use of

her incubators, and Mary Hannah and Ellie Olmos for their help processing flow cytometry samples. This work was supported by the National Science Foundation Dimensions of Biodiversity program (Award #1046297 to SDA and ACM) and Major Research Instrumentation program (Award #1126749 to ACM).

Additional supporting information is available from the online version of this article at the publisher's website.

519 **REFERENCES**

520

521 Arendt, J.D. (1997) Adaptive intrinsic growth rates: an integration across taxa. *Q. Rev. Biol.* **72**:
522 149–177.

523 Arrigo, K.R. (2005) Marine microorganisms and global nutrient cycles. *Nature* **437**: 343–8.

524 Arrigo, K.R. (1999) Phytoplankton community structure and the drawdown of nutrients and CO2
525 in the Southern Ocean. *Science* **283**: 365–367.

526 Aschar-Sobbi, R., Abramov, A.Y., Diao, C., Kargacin, M.E., Kargacin, G.J., French, R.J., and
527 Pavlov, E. (2008) High sensitivity, quantitative measurements of polyphosphate using a
528 new DAPI-based approach. *J. Fluoresc.* **18**: 859–66.

529 Aumont, O. and Bopp, L. (2006) Globalizing results from ocean in situ iron fertilization studies.
530 *Global Biogeochem. Cycles* **20**: GB2017.

531 Berdalet, E., Roldán, C., Olivar, M.P., and Lysnes, K. (2005) Quantifying RNA and DNA in
532 planktonic organisms with SYBR Green II and nucleases. Part A. Optimisation of the
533 assay. *Sci. Mar.* **69**: 1–16.

534 Blazewicz, S.J., Barnard, R.L., Daly, R.A., and Firestone, M.K. (2013) Evaluating rRNA as an
535 indicator of microbial activity in environmental communities: limitations and uses. *ISME J.*
536 **7**: 2061–2068.

537 Blomberg, S.P., Garland, T., and Ives, A.R. (2003) Testing for phylogenetic signal in
538 comparative data: Behavioral traits are more labile. *Evolution (N. Y).* **57**: 717–45.

539 Bratbak, G. (1985) Bacterial biovolume and biomass estimations. *Appl. Environ. Microbiol.* **49**:
540 1488–93.

541 Bremer, H. and Dennis, P.P. (1996) Modulation of chemical composition and other parameters
542 of the cell by growth rate. In, Neidhardt, F.C. (ed), *Escherichia coli and Salmonella*. ASM
543 Press.

544 Buitenhuis, E.T., Li, W.K.W., Lomas, M.W., Karl, D.M., Landry, M.R., and Jacquet, S. (2012)
545 Picoheterotroph (Bacter and Archaea) biomass distribution in the global ocean. *Earth Syst.*
546 *Sci. Data Discuss.* **4**: 101–106.

547 Campbell, B.J., Yu, L., Heidelberg, J.F., and Kirchman, D.L. (2011) Activity of abundant and
548 rare bacteria in a coastal ocean. *Proc. Natl. Acad. Sci. U. S. A.* **108**: 12776–81.

549 Carlson, C.A., Del Giorgio, P.A., and Herndl, G.J. (2007) Microbes and the dissipation of energy
550 and respiration: From cells to ecosystems. *Oceanography* **20**: 89–100.

Carlson, C.A., Giovannoni, S.J., Hansell, D.A., Goldberg, S.J., Parsons, R., Otero, M.P., et al. (2002) Effect of nutrient amendments on bacterioplankton production, community structure, and DOC utilization in the northwestern Sargasso Sea. *Aquat. Microb. Ecol.* **30**: 19–36.

Chan, L.-K., Newton, R.J., Sharma, S., Smith, C.B., Rayapati, P., Limardo, A.J., et al. (2012) Transcriptional changes underlying elemental stoichiometry shifts in a marine heterotrophic bacterium. *Front. Microbiol.* **3**: 159.

Chen, M. (1974) Kinetics of phosphorus absorption by *Corynebacterium bovis*. *Microb. Ecol.* **1**: 164–175.

Cherrier, J., Bauer, J.E., and Druffel, E.R.M.D. (1996) Utilization and turnover of labile dissolved organic matter by bacterial heterotrophs in eastern North Pacific surface waters. *Mar. Ecol. Prog. Ser.* **139**: 267–279.

Cho, J.-C. and Giovannoni, S.J. (2004) *Oceanicola granulosus* gen. nov., sp. nov. and *Oceanicola batsensis* sp. nov., poly-beta-hydroxybutyrate-producing marine bacteria in the order "Rhodobacterales." *Int. J. Syst. Evol. Microbiol.* **54**: 1129–36.

Cho, J.-C. and Giovannoni, S.J. (2006) *Pelagibaca bermudensis* gen. nov., sp. nov., a novel marine bacterium within the Roseobacter clade in the order Rhodobacterales. *Int. J. Syst. Evol. Microbiol.* **56**: 855–9.

Chrzanowski, T.H. and Grover, J.P. (2008) Element content of *Pseudomonas fluorescens* varies with growth rate and temperature: A replicated chemostat study addressing ecological stoichiometry. *Limnol. Oceanogr.* **53**: 1242–1251.

Connon, S.A. and Giovannoni, S.J. (2002) High-throughput methods for culturing microorganisms in very-low-nutrient media yield diverse new marine isolates. *Appl. Environ. Microbiol.* **68**: 3878–3885.

Cotner, J.B. and Biddanda, B.A. (2002) Small players, large role: Microbial influence on biogeochemical processes in pelagic aquatic ecosystems. *Ecosystems* **5**: 105–121.

Cotner, J.B., Hall, E.K., Scott, J.T., and Heldal, M. (2010) Freshwater bacteria are stoichiometrically flexible with a nutrient composition similar to seston. *Front. Microbiol.* **1**: 132.

Cotner, J.B., Makino, W., and Biddanda, B.A. (2006) Temperature affects stoichiometry and biochemical composition of *Escherichia coli*. *Microb. Ecol.* **52**: 26–33.

Danger, M., Oumarou, C., Benest, D., and Lacroix, G. (2007) Bacteria can control stoichiometry and nutrient limitation of phytoplankton. *Funct. Ecol.* **21**: 202–210.

Daufresne, T. and Loreau, M. (2001) Ecological stoichiometry, primary producer-decomposer interactions, and ecosystem persistence. *Ecology* **82**: 3069.

Ducklow, H.W. (1999) The bacterial component of the oceanic euphotic zone. *FEMS Microbiol. Ecol.* **30**: 1–10.

587 Edwards, K.F., Thomas, M.K., Klausmeier, C.A., and Litchman, E. (2012) Allometric scaling and
588 taxonomic variation in nutrient utilization traits and maximum growth rate of phytoplankton.
589 *Limnol. Oceanogr.* **57**: 554–566.

590 Elser, J.J., Acharya, K., Kyle, M., Cotner, J.B., Makino, W., Markow, T., et al. (2003) Growth
591 rate-stoichiometry couplings in diverse biota. *Ecol. Lett.* **6**: 936–943.

592 Elser, J.J., Dobberfuhl, D.R., Mackay, N.A., and Schampel, J.H. (1996) Organism size, life
593 history, and N:P stoichiometry. *Bioscience* **46**: 674–684.

594 Elser, J.J., Sterner, R.W., Gorokhova, E., Fagan, W.F., Markow, T.A., Cotner, J.B., et al. (2000)
595 Biological stoichiometry from genes to ecosystems. *Ecol. Lett.* **3**: 540–550.

596 Ettema, T.J.G. and Andersson, S.G.E. (2009) The alpha-proteobacteria: the Darwin finches of
597 the bacterial world. *Biol. Lett.* **5**: 429–32.

598 Fagerbakke, K.M., Heldal, M., and Norland, S. (1996) Content of carbon, nitrogen, oxygen,
599 sulfur and phosphorus in native aquatic and cultured bacteria. *Aquat. Microb. Ecol.* **10**: 15–
600 27.

601 Felsenstein, J. (2005) PHYLIP.

602 Follows, M.J., Dutkiewicz, S., Grant, S., and Chisholm, S.W. (2007) Emergent biogeography of
603 microbial communities in a model ocean. *Science* **315**: 1843–1846.

604 Fox, J. and Weisberg, S. (2011) An R companion to applied regression Second Edition. Sage
605 Publications, Inc.

606 Fox, J. and Weisberg, S. (2010) Nonlinear regression and nonlinear least squares in R. In, Fox,
607 J. and Weisberg, S. (eds), *An R Companion to Applied Regression, 2nd Edition*. Sage,
608 Thousand Oaks, CA.

609 Franklin, O., Hall, E.K., Kaiser, C., Battin, T.J., and Richter, A. (2011) Optimization of biomass
610 composition explains microbial growth-stoichiometry relationships. *Am. Nat.* **177**: E29–42.

611 Fukuda, R., Ogawa, H., Nagata, T., and Koike, I. (1998) Direct determination of carbon and
612 nitrogen contents of natural bacterial assemblages in marine environments. *Appl. Environ.*
613 *Microbiol.* **64**: 3352–3358.

614 Del Giorgio, P.A. and Cole, J.J. (1998) Bacterial growth efficiency in natural aquatic systems.
615 *Annu. Rev. Ecol. Syst.* **29**: 503–541.

616 Giovannoni, S.J., Tripp, H.J., Givan, S., Podar, M., Vergin, K.L., Baptista, D., et al. (2005)
617 Genome streamlining in a cosmopolitan oceanic bacterium. *Science* **309**: 1242–5.

618 Goldman, J.C., Caron, D.A., and Dennett, M.R. (1987) Regulation of gross growth efficiency
619 and ammonium regeneration in bacteria by substrate C:N ratio. *Limnol. Oceanogr.* **32**:
620 1239–1252.

621 Goldman, J.C. and Dennett, M.R. (2000) Growth of marine bacteria in batch and continuous
622 culture under carbon and nitrogen limitation. *Limnol. Oceanogr.* **45**: 789–800.

623 González, J.M. and Moran, M.A. (1997) Numerical dominance of a group of marine bacteria in
624 the alpha-subclass of the class Proteobacteria in coastal seawater. *Appl. Environ.*
625 *Microbiol.* **63**: 4237–4242.

626 Güde, H. (1985) Influence of phagotrophic processes on the regeneration of nutrients in two-
627 stage continuous culture systems. *Microb. Ecol.* **11**: 193–204.

628 Hardwick, E.O., Ye, W., Moran, M.A., and Hodson, R.E. (2003) Temporal dynamics of three
629 culturable gamma-Proteobacteria taxa in salt marsh sediments. *Aquat. Ecol.* **37**: 55–64.

630 Harold, F.M. (1966) Inorganic polyphosphates in biology: Structure, metabolism, and function.
631 *Bacteriol. Rev.* **30**: 772–94.

632 Hochstädter, S. (2000) Seasonal changes of C:P ratios of seston, bacteria, phytoplankton and
633 zooplankton in a deep, mesotrophic lake. *Freshw. Biol.* **44**: 453–463.

634 Jeffrey, W.H., Von Haven, R., Hoch, M.P., and Coffin, R.B. (1996) Bacterioplankton RNA, DNA,
635 protein content and relationships to rates of thymidine and leucine incorporation. *Aquat.*
636 *Microb. Ecol.* **10**: 87–95.

637 Karl, D.M., Bjorkman, K.M., Dore, J.E., Fujieki, L., Hebel, D. V, Houlihan, T., et al. (2001)
638 Ecological nitrogen-to-phosphorus stoichiometry at station ALOHA. *Deep Sea Res. Part II*
639 *Top. Stud. Oceanogr.* **48**: 1529–1566.

640 Kembel, S.W., Cowan, P.D., Helmus, M.R., Cornwell, W.K., Morlon, H., Ackerly, D.D., et al.
641 (2010) Picante: R tools for integrating phylogenies and ecology. *Bioinformatics* **26**: 1463–4.

642 Kemp, P.F., Lee, S., and Laroche, J. (1993) Estimating the growth rate of slowly growing marine
643 bacteria from RNA content. *Appl. Environ. Microbiol.* **59**: 2594–601.

644 Kerkhof, L. and Ward, B.B. (1993) Comparison of nucleic acid hybridization and fluorometry for
645 measurement of the relationship between RNA/DNA ratio and growth rate in a marine
646 bacterium. *Appl. Environ. Microbiol.* **59**: 1303–9.

647 Kirchman, D.L. (2012) Elements, biochemicals, and structures of microbes. In, *Processes in*
648 *Microbial Ecology*. Oxford University Press, Oxford, pp. 19–34.

649 Kirchman, D.L. (1990) Limitation of bacterial growth by dissolved organic matter in the subarctic
650 Pacific. *Mar. Ecol. Prog. Ser.* **62**: 47–54.

651 Kirchman, D.L. (2008) Microbial Ecology of the Oceans, Second Edition Kirchman, D.L. (ed)
652 John Wiley & Sons, Inc., Hoboken, New Jersey.

653 Kirchman, D.L. (2000) Uptake and regeneration of inorganic nutrients by marine heterotrophic
654 bacteria. In, Kirchman, D.L. (ed), *Microbial Ecology of the Oceans, First Edition*. Wiley-Liss,
655 New York, pp. 261–288.

Kirchman, D.L., Meon, B., Cottrell, M.T., Hutchins, D., Weeks, D., and Bruland, K.W. (2000) Carbon versus iron limitation of bacterial growth in the California upwelling regime. *Limnol. Oceanogr.* **45**: 1681–1688.

Klausmeier, C.A., Litchman, E., Daufresne, T., and Levin, S.A. (2004) Optimal nitrogen-to-phosphorus stoichiometry of phytoplankton. *Nature* **429**: 171–174.

Klausmeier, C.A., Litchman, E., Daufresne, T., and Levin, S.A. (2008) Phytoplankton stoichiometry. *Ecol. Res.* **23**: 479–485.

Kornberg, A., Rao, N.N., and Ault-Riche, D. (1999) Inorganic polyphosphate: A molecule of many functions. *Annu. Rev. Biochem.* **68**: 89–125.

Lomas, M.W., Burke, A.L., Lomas, D.A., Bell, D.W., Shen, C., Dyhrman, S.T., and Ammerman, J.W. (2010) Sargasso Sea phosphorus biogeochemistry: an important role for dissolved organic phosphorus (DOP). *Biogeosciences* **7**: 695–710.

Løvdal, T., Skjoldal, E.F., Heldal, M., Norland, S., and Thingstad, T.F. (2008) Changes in morphology and elemental composition of *Vibrio splendidus* along a gradient from carbon-limited to phosphate-limited growth. *Microb. Ecol.* **55**: 152–61.

Makino, W. and Cotner, J.B. (2004) Elemental stoichiometry of a heterotrophic bacterial community in a freshwater lake: implications for growth- and resource-dependent variations. *Aquat. Microb. Ecol.* **34**: 33–41.

Makino, W., Cotner, J.B., Sterner, R.W., and Elser, J.J. (2003) Are bacteria more like plants or animals? Growth rate and resource dependence of bacterial C:N:P stoichiometry. *Funct. Ecol.* **17**: 121–130.

Marie, D., Partensky, F., Vaulot, D., and Brussaard, C. (2001) Enumeration of phytoplankton, bacteria, and viruses in marine samples. *Curr. Protoc. Cytom.* 10:11.11.1–11.11.15.

Martinussen, I. and Thingstad, T.F. (1987) Utilization of N, P and organic C by heterotrophic bacteria. II. Comparison of experiments and a mathematical model. *Mar. Ecol. Prog. Ser.* **37**: 285–293.

Martiny, A.C., Coleman, M.L., and Chisholm, S.W. (2006) Phosphate acquisition genes in *Prochlorococcus* ecotypes: evidence for genome-wide adaptation. *Proc. Natl. Acad. Sci. U. S. A.* **103**: 12552–7.

Martiny, A.C., Pham, C.T.A., Primeau, F.W., Vrugt, J.A., Moore, J.K., Levin, S.A., and Lomas, M.W. (2013a) Strong latitudinal patterns in the elemental ratios of marine plankton and organic matter. *Nat. Geosci.* **6**: 279-283.

Martiny, A.C., Treseder, K.K., and Pusch, G.D. (2013b) Phylogenetic conservatism of functional traits in microorganisms. *ISME J.* **7**: 830–8.

Michaels, A.F., Karl, D.M., and Capone, D.G. (2001) Element stoichiometry, new production and nitrogen fixation. *Oceanography* **14**: 68–77.

692 Moore, J.K., Doney, S.C., and Lindsay, K. (2004) Upper ocean ecosystem dynamics and iron
693 cycling in a global three-dimensional model. *Global Biogeochem. Cycles* **18**: GB4028.

694 Van Mooy, B.A.S., Fredricks, H.F., Pedler, B.E., Dyhrman, S.T., Karl, D.M., Koblízek, M., et al.
695 (2009) Phytoplankton in the ocean use non-phosphorus lipids in response to phosphorus
696 scarcity. *Nature* **458**: 69–72.

697 Moran, M.A., Buchan, A., González, J.M., Heidelberg, J.F., Whitman, W.B., Kiene, R.P., et al.
698 (2004) Genome sequence of *Silicibacter pomeroyi* reveals adaptations to the marine
699 environment. *Nature* **432**: 910–3.

700 Neidhardt, F.C. and Magasanik, B. (1960) Studies on the role of ribonucleic acid in the growth of
701 bacteria. *Biochim. Biophys. Acta* **42**: 99–116.

702 Pinheiro, J. and Bates, D. SSlogis.

703 Pomeroy, L.R., Williams, P.J. leB, Azam, F., and Hobbie, J.E. (2007) The Microbial Loop.
704 *Oceanography* **20**: 28–33.

705 Poulsen, L.K., Ballard, G., and Stahl, D.A. (1993) Use of rRNA fluoresence in situ hybridization
706 for measuring the activity of single cells in young and established biofilms. *Appl. Environ.*
707 *Microbiol.* **59**: 1354–1360.

708 Pruesse, E., Peplies, J., and Glöckner, F.O. (2012) SINA: accurate high-throughput multiple
709 sequence alignment of ribosomal RNA genes. *Bioinformatics* **28**: 1823–9.

710 Pruesse, E., Quast, C., Knittel, K., Fuchs, B.M., Ludwig, W., Peplies, J., and Glöckner, F.O.
711 (2007) SILVA: a comprehensive online resource for quality checked and aligned ribosomal
712 RNA sequence data compatible with ARB. *Nucleic Acids Res.* **35**: 7188–96.

713 Quast, C., Pruesse, E., Yilmaz, P., Gerken, J., Schweer, T., Yarza, P., et al. (2013) The SILVA
714 ribosomal RNA gene database project: improved data processing and web-based tools.
715 *Nucleic Acids Res.* **41**: D590–6.

716 Quigg, A., Finkel, Z. V, Irwin, A.J., Rosenthal, Y., Ho, T.-Y., Reinfelder, J.R., et al. (2003) The
717 evolutionary inheritance of elemental stoichiometry in marine phytoplankton. *Nature* **425**:
718 291–4.

719 Quigg, A., Irwin, A.J., and Finkel, Z. V (2011) Evolutionary inheritance of elemental
720 stoichiometry in phytoplankton. *Proc. R. Soc. B Biol. Sci.* **278**: 526–34.

721 R Core Team. (2012) R: A language and environment for statistical computing. *R Found. Stat.*
722 *Comput.*

723 Rappé, M.S., Connon, S.A., Vergin, K.L., and Giovannoni, S.J. (2002) Cultivation of the
724 ubiquitous SAR11 marine bacterioplankton clade. *Nature* **418**: 630–3.

Redfield, A.C. (1934) On the proportions of organic derivatives in sea water and their relation to the composition of plankton. In, Daniel, R.J. (ed), *James Johnstone Memorial Volume*. University Press of Liverpool, pp. 177–192.

Redfield, A.C. (1958) The biological control of chemical factors in the environment. *Am. Sci.* **46**: 205–221.

Rhee, G.-Y. (1978) Effects of N:P atomic ratios and nitrate limitation on algal growth, cell composition, nitrate uptake. *Limnol. Oceanogr.* **23**: 10–25.

Rosset, R., Julien,J., and Monier, R. (1966) Ribonucleic acid composition of bacteria as a function of growth rate. *J. Mol. Biol.* **18**: 308–320.

Shannon, S.P., Chrzanowski, T.H., and Grover,J.P. (2007) Prey food quality affects flagellate ingestion rates. *Microb. Ecol.* **53**: 66–73.

Simon, M. and Azam, F. (1989) Protein content and protein synthesis rates of planktonic marine bacteria. *Mar. Ecol. Prog. Ser.* **51**: 201–213.

Solorzano, L. and Sharp, J.H. (1980) Determination of total dissolved phosphorus and particulate phosphorus in natural water. *Limnol. Oceanogr.* **25**: 754–758.

Sterner, R.W. and Elser, J.J. (2002) Ecological stoichiometry: The biology of elements from molecules to the biosphere Princeton University Press, Princeton.

Tezuka, Y. (1990) Bacterial regeneration of ammonium and phosphate as affected by the carbon:nitrogen:phosphorus ratio of organic substrates. *Microb. Ecol.* **19**: 227–238.

Vollmer, W., Blanot, D., and de Pedro, M.A. (2008) Peptidoglycan structure and architecture. *FEMS Microbiol. Rev.* **32**: 149–67.

Vrede, K., Heldal, M., Norland, S., and Bratbak, G. (2002) Elemental composition (C, N, P) and cell volume of exponentially growing and nutrient-limited bacterioplankton. *Appl. Environ. Microbiol.* **68**: 2965.

Vrede, T., Dobberfuhl, D.R., Kooijman, S.A.L.M., and Elser, J.J. (2004) Fundamental connections among organism C:N:P stoichiometry, macromolecular composition, and growth. *Ecology* **85**: 1217–1229.

Wagner, R. (1994) The regulation of ribosomal RNA synthesis and bacterial cell growth. *Arch. Microbiol.* 100–109.

Weber, T.S. and Deutsch, C. (2010) Ocean nutrient ratios governed by plankton biogeography. *Nature* **467**: 550–554.

Zubkov, M. V, Fuchs, B.M., Eilers, H., Burkill, P.H., and Amann, R. (1999) Determination of total protein content of bacterial cells by SYPRO staining and flow cytometry. *Appl. Environ. Microbiol.* **65**: 3251–7.

760 ***FIGURE LEGENDS***

761

762 ***Figure 1.*** Phylogenetic relationships between the bacterial strains used in this study inferred by
763 maximum likelihood estimation from 16S rRNA gene sequence comparisons. Bars show
764 taxonomic associations at the family level with genus names on the right. Three archaeal
765 sequences, including *Thermoproteus tenax*, *Sulfolobus solataricus*, and *Methanococcus*
766 *vannielii*, were used as an outgroup. Values at the nodes show the bootstrap support from 100
767 resampled data sets. Scale bar represents branch length.

768

769 ***Figure 2.*** Elemental composition of marine bacteria in this study. Median values for each strain
770 are shown along with the quartiles, minimum, and maximum values. Geometric means are
771 given in Table 1. Dashed red lines depict Redfield ratios for (a) C:P = 106, (b) N:P = 16, or (c)
772 C:N = 6.625. Solid black lines and shaded areas show estimated median ratios across all
773 strains ± 95% CI. Overall, bacterial N:P was equal to Redfield ($p = 0.424$, Wilcoxon test), but
774 C:P ($p = 0.048$) and C:N ($p = 0.001$) ratios were significantly different. No significant
775 phylogenetic signal was detected for any of the ratios. Results of Kruskal-Wallis ANOVAs
776 indicated significant variance in all ratios among the strains ($p < 0.001$).

777

778 ***Figure 3.*** Strain-specific growth rates of marine bacteria in this study. Median values for each
779 strain are shown along with the quartiles, minimum, and maximum values. Means are given in
780 Table 1. Blomberg's K statistic for phylogenetic signal was not significant ($K = 0.045$, $p = 0.693$).
781 Results of a Kruskal-Wallis ANOVA indicated significant variance in growth rate among the
782 strains ($p < 0.001$).

783

784 ***Figure 4.*** Allocation to (a) DNA, (b) RNA, and (c) protein (normalized to C biomass, w/w) of
785 marine bacteria in this study. Median values for each strain are shown along with the quartiles,

786 minimum, and maximum values. Means are given in Table S1. Blomberg's K statistic for
787 phylogenetic signal was significant for DNA (K = 0.275, p = 0.007) and protein content (K =
788 0.602, p = 0.001), but not RNA (K = 0.050, p = 0.594). Results of Kruskal-Wallis ANOVAs
789 indicated significant variance in all traits among the strains (p < 0.001).
790
791 ***Figure 5.*** Contribution of RNA-P to total biomass P of marine bacteria in this study. Median
792 values for each strain are shown along with the quartiles, minimum, and maximum values.
793 Means are given in Table 1. Blomberg's K statistic for phylogenetic signal was not significant (K
794 = 0.088, p = 0.404). Dotted line equals 1.
795
796 ***Figure 6.*** Relationships between (a) C:P and (b) N:P elemental composition and growth rate, or
797 (c) P and (d) RNA content (normalized to C biomass, w/w) and growth rate for strains of marine
798 bacteria in this study. Points represent the arithmetic mean ± sem for each strain, except ratios
799 are shown as geometric means. Shapes depict different families. Spearman's rank correlation
800 indicated a significant association between RNA content and growth rate (p = 0.05, *rho* = 0.59),
801 but no significant associations were detected between C:P (p = 0.94) or N:P (p = 0.68) ratios
802 and growth rate or between P (p = 0.94) content and growth rate.
803
804

SUPPORTING INFORMATION

Figure S1. Allocation to (a) DNA, (b) RNA, and (c) protein (normalized to cell abundance) of marine bacteria in this study. Median values for each strain are shown along with the quartiles, minimum, and maximum values. Means are given in Table 1. Blomberg's K statistic for phylogenetic signal was not significant.

Figure S2. (a) P and (b) RNA content (normalized to cell count) plotted in relation to growth rate for strains of marine bacteria in this study. Points represent the mean ± sem for each strain. Shapes depict different families. Spearman's rank correlation indicated a significant association between RNA content and growth rate ($p = 0.05$, *rho* = 0.58), but not P content and growth rate ($p = 0.15$).

Figure S3. Addition and recovery of pure (a) DNA, (b) RNA, or (c) protein to cell lysate from *Roseovarius* sp. TM1035. Points represent the means ± sem from triplicate determinations. Detection values have been adjusted for the baseline signal from unamended cell lysate.

Table S1. Comparison of mean growth rate and macromolecule content normalized to carbon (C) biomass (w/w) for strains of marine bacteria in this study.

Table S2. Components of standard seawater media (SSM).

Table S3. Comparison of Wilcoxon signed rank tests for departures from Redfield ratios[1] between all strains and the subset of strains in exponential growth.

Table S4. Comparison of phylogenetic signal between all strains and the subset of strains in exponential growth.

Table S5. Calculated DNA extraction efficiency based on genome size.

Table S6. SN trace metal stock solution used for preparation of isolation media and SSM.

TABLE 1. Comparison of mean[1] growth rate, cellular macromolecule content, RNA:DNA ratio, % total phosphorus (P) in RNA, cellular C, N and P quotas, and molar element ratios for strains of marine bacteria in this study.

Isolate	N	Growth rate (hr^{-1})	Macromolecule[2] ($fg\ cell^{-1}$)			RNA:DNA ratio	% P from RNA	Element quota ($fg\ cell^{-1}$)			Molar ratio		
			DNA	RNA	Protein			C	N	P	C:N	C:P	N:P
HTCC1062	6	0.009	NA[3]	NA	NA	NA	NA	32.2	NA	2.9	NA	36	NA
DSS-3	5	0.210	2.56	27.4	62.9	10.7	99.3%	142	25.1	2.6	6.61	141	21
HTCC2516	6	0.125	1.88	9.33	30.5	4.9	19.8%	94.8	21.7	4.4	5.12	55	11
HTCC2601	6	0.293	3.21	30.0	78.5	9.1	74.0%	172	35.9	3.7	5.56	121	22
Alt1C	6	0.323	3.65	12.3	71.4	3.4	19.8%	88.6	25.3	5.8	4.08	39	9.6
Vib1A	6	0.621	3.08	6.35	66.6	2.1	11.0%	129	34.1	5.4	4.42	62	14
Vib2D	4	0.200	2.39	3.02	66.2	1.3	9.1%	168	26.8	3.1	7.35	139	19
Oce241	4	0.233	2.48	4.10	53.9	1.7	16.3%	86.0	21.7	2.4	4.63	94	20
Oce340	4	0.246	6.66	64.8	129	9.5	103%	203	51.4	5.9	4.60	89	19
Mor224	4	0.225	2.85	9.64	71.9	3.3	6.3%	292	74.3	14	4.57	54	12
Mor119	4	0.041	0.65	0.55	41	0.86	1.3%	163	48.9	4.1	4.08	103	25
Hal005	5	0.332	4.53	41.3	143.4	9.1	72.1%	190	49.8	5.6	4.47	92	21
Hal146	5	0.088	2.87	4.14	97.4	1.5	7.7%	127	33.7	5.0	4.40	65	15
Grand Mean		0.227	3.07	17.7	76	4.8	37%	145	37.4	5.0	4.91	77	17

[1]Values shown represent arithmetic means, except geometric means are reported for the elemental ratios.
[2]Macromolecule mass based on standard curve concentrations of λ dsDNA, *E. coli* rRNA, or BSA protein.
[3]NA, value was below detection.

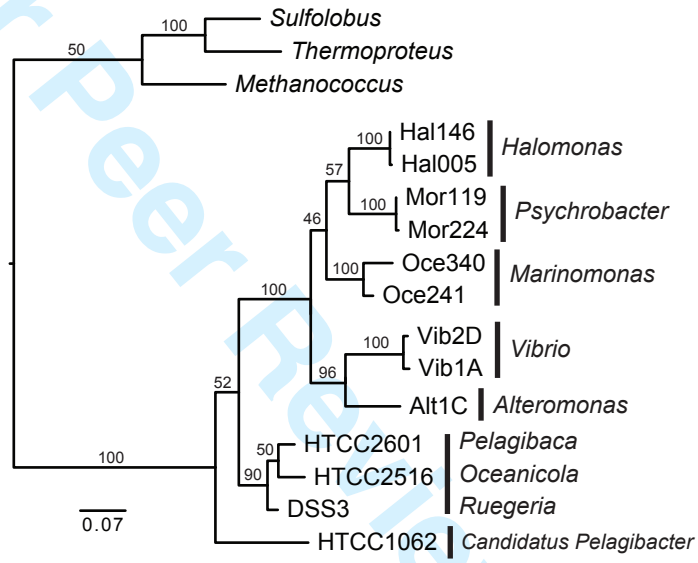

Figure 1

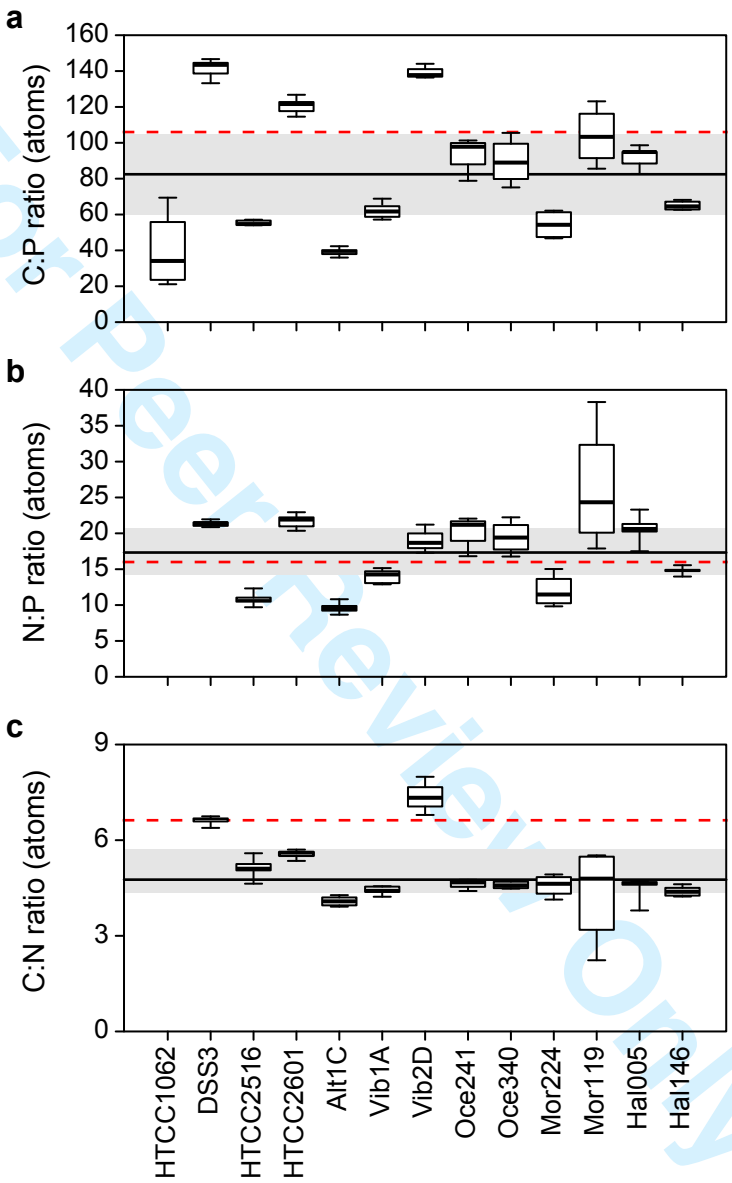

Figure 2

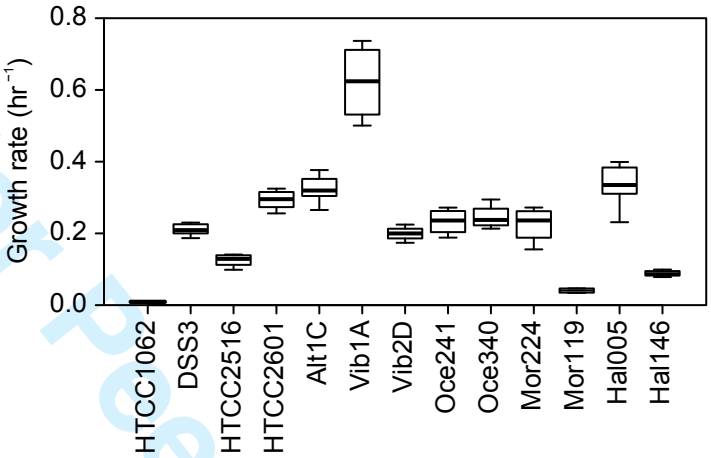

Figure 3

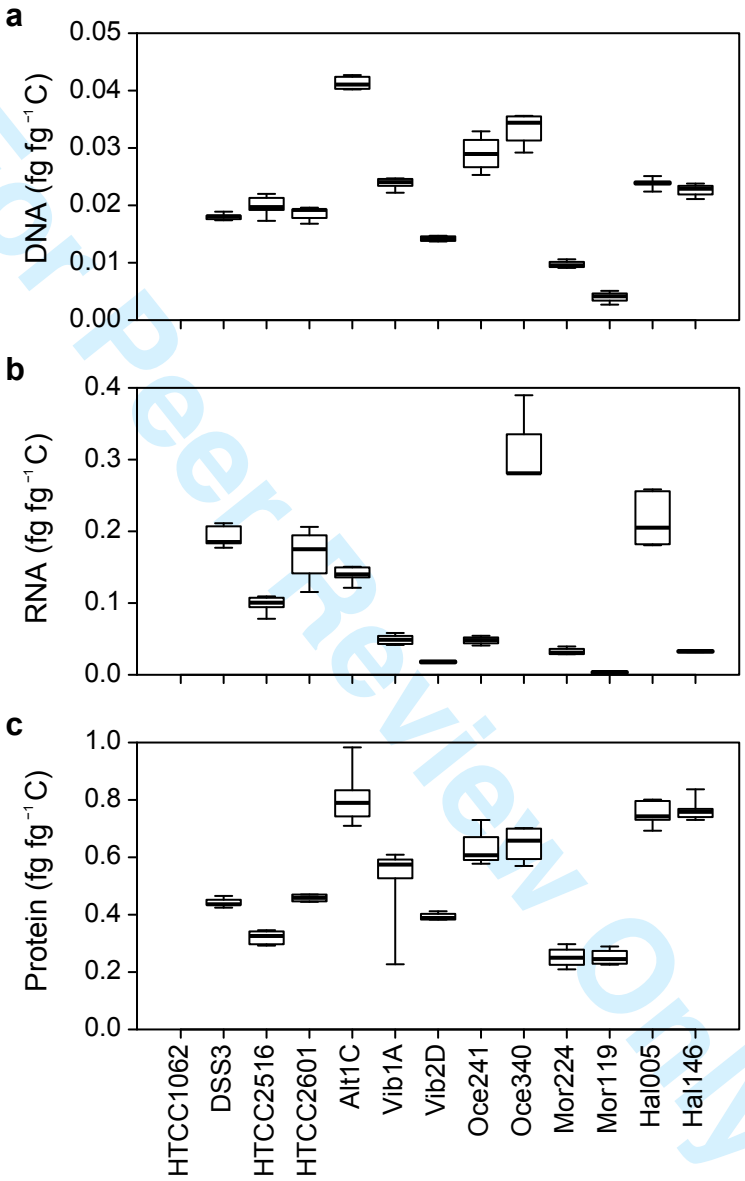

Figure 4

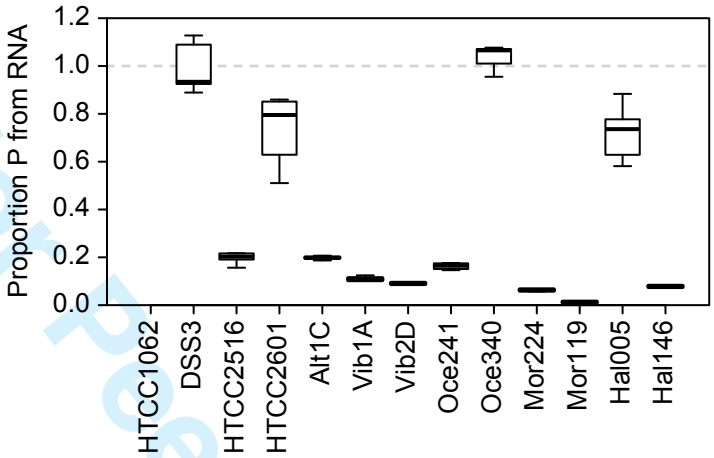

Figure 5

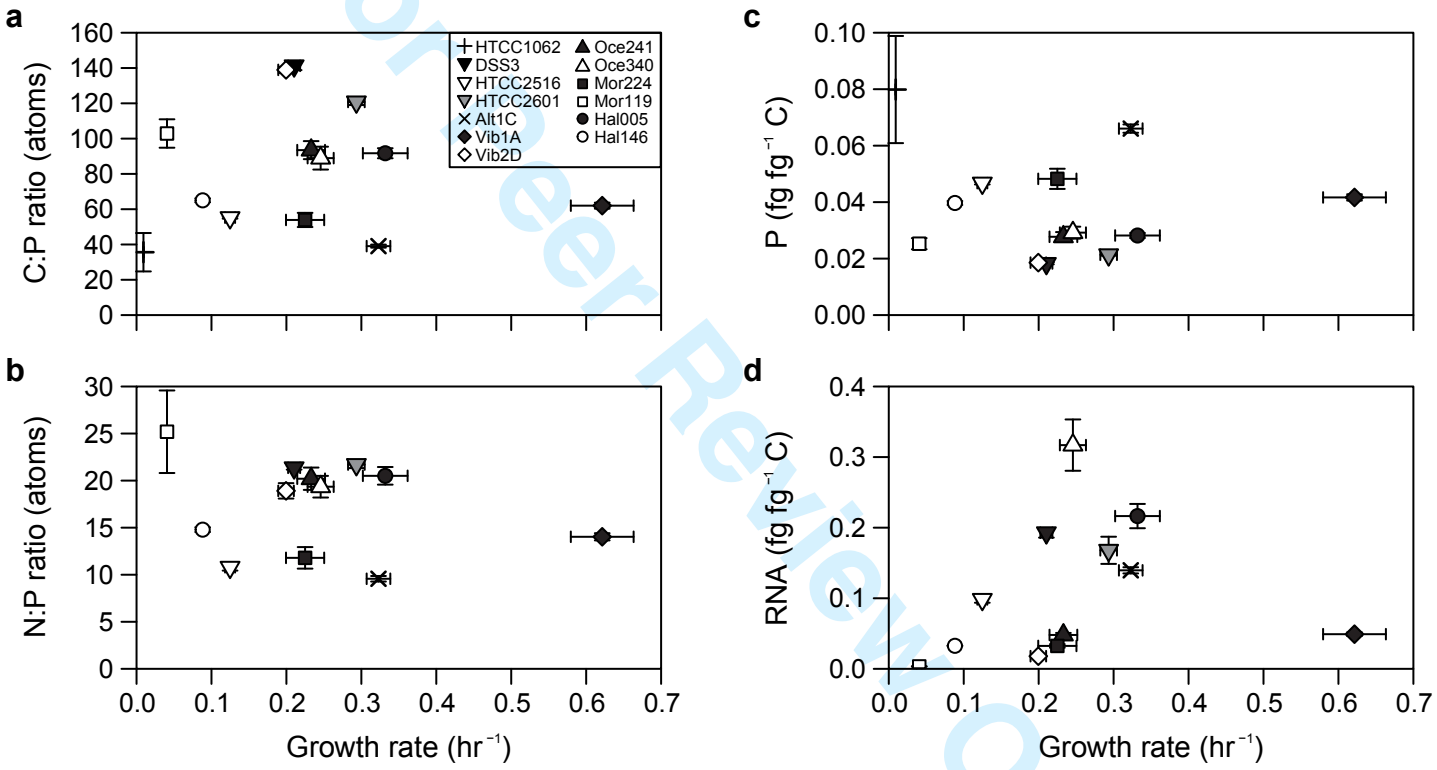

Figure 6

Supporting Information: Methods

EXPERIMENTAL PROCEDURES

BACTERIAL ISOLATION AND IDENTIFICATION

Bacteria were received from collaborators (strains HTCC1062, DSS-3, HTCC2516, and HTCC2601; Rappé et al., 2002; Moran et al., 2004; Cho and Giovannoni, 2004, 2006) or isolated from coastal seawater collected at Newport Pier, Newport Beach, CA, USA (33°36'25"N, 117°55'48"W) in July 2009, September 2009, November 2009, or January 2010. Seawater samples for isolation were serially diluted and plated on 1.5% agar medium made of filtered (0.2-μm), autoclaved seawater amended with 0.883 mM $NaNO_3$, 50 μM NaH_2PO_4, 13.43 μM Na_2-EDTA, SN trace metals (10^{-3} dilution of stock; Table S6), and 1mM adenosine-5'-monophosphate or asparagine (final concentration). Plates were incubated in ambient light at room temperature for 2-4 weeks, after which colonies were selected for further isolation. Single colonies were transferred three times on the same agar medium to ensure purity, and then inoculated into half-strength YTSS liquid media (González and Moran, 1997; Hardwick et al., 2003) for propagation and preservation in 15% glycerol at -80°C. Strains DSS-3, HTCC2516, and HTCC2601 were maintained in ½YTSS medium at room temperature upon receipt and preserved in the same manner. Strain HTCC1062 was propagated in low-nutrient heterotrophic media (LNHM; Connon and Giovannoni, 2002) prepared from filtered, autoclaved seawater collected at the San Pedro Ocean Time-Series Station (SPOTS; 33°33′00"N, 118°24′00"W). LNHM was amended with 95 μM Na_2CO_3 to restore the bicarbonate buffer, a mix of vitamins (10^{-4} dilution of stock, Rappé et al., 2002), 100 nM L-methionine (as in Tripp et al., 2008), 10 μM NH_4Cl, 1 μM K_2HPO_4, and 0.001% (w/v) each D-glucose, sodium acetate, and glycerol. HTCC1062 was acclimated to growth at 20°C and preserved in 15% glycerol at -80°C. All glassware for media preparation and culturing was acid washed (10% HCl) and all media components were sterilized by autoclaving (121°C for 20 min L^{-1}) or filtering where appropriate.

Supporting Information: Methods

Bacteria isolated from Newport Beach, CA, were identified by 16S ribosomal RNA (rRNA) gene sequences. Genomic DNA was isolated from overnight cultures of each bacterial strain using an UltraClean Microbial DNA Isolation kit (MoBio, San Diego, CA, USA) and served as template for PCR targeting the near-complete 16S rRNA gene with primers pA forward (5'-AGA GTT TGA TCC TGG CTC AG-3') and pH reverse (5'-AAG GAG GTG ATC CAG CCG CA-3') (Edwards et al., 1989). PCR products were purified using a NucleoSpin Extract II kit (Macherey-Nagel, Düren, Germany) and sequenced with the same primers by Laragen, Inc. (Culver City, CA, USA) on an ABI Prism 3730 Genetic Analyzer (Applied Biosystems, Foster City, CA, USA). Consensus sequences were taxonomically classified using the SINA alignment service from the Silva rRNA database (http://beta.arb-silva.de/aligner/; Pruesse et al., 2012). Nucleotide sequences have been deposited in the GenBank database under accession numbers KC990022-KC990031.

ANALYTICAL METHODS: MACROMOLECULE CONTENT

Nucleic acids and proteins were released from filter samples in a solution of Tris buffer (5 mM Tris, pH 8.0, Ambion) and RNA preservative (nucleic acid samples only; saturated ammonium sulfate solution of 0.5M EDTA, 1M sodium citrate, and 700 g L^{-1} ammonium sulfate). Samples were mechanically lysed using a MP FastPrep-24 bead beater (MP Biomedicals, Santa Ana, CA, USA) at 5.5 m/s for 2 minutes in 1-minute increments, incubating the samples on ice for 5 minutes in between. The supernatant was collected for analysis after centrifugation (10,000 x *g* for 4 minutes) at 4°C to pellet cell and filter debris. Three identical 96-well microplates were prepared for every assay, one for detection of each macromolecule. Pre-diluted standards included with each kit were further diluted with supernatant from media blanks to bracket expected concentrations of each macromolecule (0-250 ng mL^{-1} λ dsDNA, 0-500 ng mL^{-1} *E. coli* rRNA, and 0-5 µg mL^{-1} BSA protein). Each fluorophore was diluted 1:200 in the appropriate buffer and added to triplicate wells of samples and standards. Plates were

incubated at room temperature in the dark for 3 or 15 minutes (for nucleic acids and proteins, respectively) prior to measuring fluorescence at the specified excitation and emission values on a Biotek Synergy4 microplate reader (BioTek, Winooski, VT, USA).

Macromolecule concentrations were calculated based on standard curve regressions of fluorescence vs. known standard concentrations (λ dsDNA, *E. coli* rRNA, or BSA protein). DNA standards were linear, while an asymptotic regression model best described RNA standards, and an exponential regression model best described protein standards. The limit of detection for each macromolecule was estimated as the mean of triplicate determinations from background media (blank) samples plus 3 times the standard deviation. The limit of detection for DNA in our assays was 0.41 ± 0.18 ng, RNA was 2.3 ± 0.98 ng, and protein was 67.4 ± 24.1 ng. We also calculated the coefficient of variation (CV) for each macromolecule as the ratio of the standard deviation to the mean of triplicate determinations from all values of the standard curves. For our assays, the CV for DNA was 3.2 ± 0.8%, RNA was 3.8 ± 1.7%, and protein was 4.8 ± 1.4%. All sample protein concentrations were divided by a quench coefficient of 0.2862, which was the slope of the observed vs. expected values for the Mor224 spiked controls averaged over all assays (n = 6). Only the 2 closest analytical replicates were used to determine the mean macromolecular content for each sample. Extraction efficiency for DNA using this assay was estimated at ~50%, based on the known genome sizes of DSS-3, HTCC2516, and HTCC2601 (http://www.roseobase.org), assuming one genome per cell and 100% retention of cells on the filter (Table S5); however, the nucleic acid and protein values reported were not corrected for this estimation.

Supporting Information: Methods

REFERENCES

Cho, J.-C. and Giovannoni, S.J. (2004) *Oceanicola granulosus* gen. nov., sp. nov. and *Oceanicola batsensis* sp. nov., poly-beta-hydroxybutyrate-producing marine bacteria in the order "Rhodobacterales." *Int. J. Syst. Evol. Microbiol.* **54**: 1129–36.

Cho, J.-C. and Giovannoni, S.J. (2006) *Pelagibaca bermudensis* gen. nov., sp. nov., a novel marine bacterium within the Roseobacter clade in the order Rhodobacterales. *Int. J. Syst. Evol. Microbiol.* **56**: 855–9.

Connon, S.A. and Giovannoni, S.J. (2002) High-throughput methods for culturing microorganisms in very-low-nutrient media yield diverse new marine isolates. *Appl. Environ. Microbiol.* **68**: 3878–3885.

Edwards, U. et al. (1989) Isolation and direct complete nucleotide determination of entire genes. Characterization of a gene coding for 16S ribosomal RNA. *Nucleic Acids Res.* **17**: 7843–7853.

González, J.M. and Moran, M.A. (1997) Numerical dominance of a group of marine bacteria in the alpha-subclass of the class Proteobacteria in coastal seawater. *Appl. Environ. Microbiol.* **63**: 4237–4242.

Hardwick, E.O. et al. (2003) Temporal dynamics of three culturable gamma-Proteobacteria taxa in salt marsh sediments. *Aquat. Ecol.* **37**: 55–64.

Moran, M.A. et al. (2004) Genome sequence of *Silicibacter pomeroyi* reveals adaptations to the marine environment. *Nature* **432**: 910–3.

Pruesse, E. et al. (2012) SINA: accurate high-throughput multiple sequence alignment of ribosomal RNA genes. *Bioinformatics* **28**: 1823–9.

Rappé, M.S. et al. (2002) Cultivation of the ubiquitous SAR11 marine bacterioplankton clade. *Nature* **418**: 630–3.

Tripp, H.J. et al. (2008) SAR11 marine bacteria require exogenous reduced sulphur for growth. *Nature* **452**: 741–4.

Supporting Information: Tables

TABLE S1. Comparison of mean growth rate and macromolecule content normalized to carbon (C) biomass (w/w) for strains of marine bacteria in this study.

Isolate	N	Growth rate (hr^{-1})	Macromolecule[1] ($fg\ fg^{-1}$ C)		
			DNA	RNA	Protein
HTCC1062	6	0.009	NA[2]	NA	NA
DSS-3	5	0.210	0.018	0.19	0.44
HTCC2516	6	0.125	0.020	0.10	0.32
HTCC2601	6	0.293	0.019	0.17	0.46
Alt1C	6	0.323	0.041	0.14	0.81
Vib1A	6	0.621	0.024	0.049	0.52
Vib2D	4	0.200	0.014	0.018	0.39
Oce241	4	0.233	0.029	0.048	0.63
Oce340	4	0.246	0.033	0.38	0.65
Mor224	4	0.225	0.010	0.032	0.25
Mor119	4	0.041	0.004	0.003	0.25
Hal005	5	0.332	0.024	0.27	0.75
Hal146	5	0.088	0.023	0.033	0.77
Grand Mean		0.228	0.022	0.11	0.52

[1]Macromolecule mass based on standard curve concentrations of λ dsDNA, *E. coli* rRNA, or BSA protein.
[2]NA, value was below detection.

TABLE S2. Standard seawater media (SSM).

Compound	Molecular Formula	Concentration (L^{-1})	Element (L^{-1})
Sodium acetate	$C_2H_3NaO_2$	87.5 µmol	175 µmol C
D-Glucose	$C_6H_{12}O_6$	29.17 µmol	175 µmol C
Glycerol	$C_3H_8O_3$	58.35 µmol	175 µmol C
Ammonium chloride	NH_4Cl	80 µmol	80 µmol N
Potassium phosphate dibasic	K_2HPO_4	5 µmol	5 µmol P
L-Methionine	$C_5H_{11}NO_2S$	100 nmol	
EDTA disodium salt dihydrate	$C_{10}H_{14}N_2Na_2O_8 \cdot 2H_2O$	15 µmol	
Sodium carbonate	Na_2CO_3	95 µmol	
SN trace metals (Table S2)		1 mL	
Vitamins (Table S5)		0.1 mL	

Supporting Information: Tables

TABLE S3. Comparison of Wilcoxon signed rank tests for departures from Redfield ratios[1] between all strains and the subset of strains in exponential growth.

Dataset	Ratio	One-sided test	P (two-sided)	P (one-sided)	Median	95%CI	
All strains	C:N	less than Redfield	0.001	0.001	4.76	4.36	5.72
Exponential only	C:N	less than Redfield	0.016	0.008	4.82	4.33	5.99
All strains	C:P	less than Redfield	0.048	0.024	82.5	60.1	104.9
Exponential only	C:P	less than Redfield	0.098	0.049	79.1	46.5	114.0
All strains	N:P	NA	0.424	NA	17.3	14.2	20.8
Exponential only	N:P	NA	0.844	NA	17.1	10.8	22.3

[1]Redfield C:N = 6.625, C:P = 106, N:P = 16

TABLE S4. Comparison of phylogenetic signal between all strains and the subset of strains in exponential growth.

Trait	All strains		Exponential only	
	K	P	K	P
Protein (fg/fg C)	0.602	0.001	0.755	0.011
DNA (fg/fg C)	0.275	0.007	0.361	0.070
Proportion P in DNA	0.195	0.071	0.657	0.028
C:N ratio	0.160	0.339	0.350	0.135
N (fg/fg C)	0.127	0.329	0.111	0.525
P (fg/fg C)	0.095	0.304	0.131	0.477
Proportion P in RNA	0.088	0.404	0.311	0.281
N (fg/cell)	0.073	0.493	0.084	0.613
Protein (fg/cell)	0.066	0.445	0.097	0.561
C (fg/cell)	0.061	0.652	0.071	0.751
RNA:DNA ratio	0.059	0.589	0.183	0.446
DNA (fg/cell)	0.053	0.543	0.074	0.687
C:P ratio	0.053	0.423	0.075	0.601
RNA (fg/fg C)	0.050	0.594	0.267	0.212
Growth Rate (hr)	0.045	0.693	0.057	0.682
RNA (fg/cell)	0.041	0.677	0.198	0.504
N:P ratio	0.028	0.862	0.026	0.923
P (fg/cell)	0.027	0.789	0.023	0.883

Supporting Information: Tables

TABLE S5. Calculated DNA extraction efficiency based on genome size.

Strain	Genome size (bp)	Expected DNA (fg/genome)	Measured DNA (fg/cell)	Extraction efficiency[1]
DSS-3	4,109,442 + 491,611	5.04	2.56	50.8%
HTCC2516	4,039,111	4.43	1.88	42.5%
HTCC2601	5,425,920	5.95	3.21	54.0%

[1]Assuming 100% cells retained on filter and 1 genome/cell

TABLE S6. SN trace metal stock solution used for preparation of isolation media and SSM.

Compound	Molecular Formula	Concentration (L^{-1})
Zinc sulfate heptahydrate	$ZnSO_4 \cdot 7H_2O$	0.772 mmol
Manganese(II) chloride tetrahydrate	$MnCl_2 \cdot 4H_2O$	7.07 mmol
Cobalt(II) chloride hexahydrate	$CoCl_2 \cdot 6H_2O$	0.086 mmol
Sodium molybdate dihydrate	$Na_2MoO_4 \cdot 2H_2O$	1.61 mmol
Citric acid monohydrate	$C_6H_8O_7 \cdot H_2O$	29.7 mmol
Ammonium iron(III) citrate	$C_6H_8O_7 \cdot xFe_3^+ \cdot yNH_3$	22.6 mmol

Supporting Information: Figure Legends

FIGURE LEGENDS

Figure S1. Allocation to (a) DNA, (b) RNA, and (c) protein (normalized to cell abundance) of marine bacteria in this study. Median values for each strain are shown along with the quartiles, minimum, and maximum values. Means are given in Table 1. Blomberg's K statistic for phylogenetic signal was not significant.

Figure S2. (a) P and (b) RNA content (normalized to cell count) plotted in relation to growth rate for strains of marine bacteria in this study. Points represent the mean ± sem for each strain. Shapes depict different families. Spearman's rank correlation indicated a significant association between RNA content and growth rate ($p = 0.05$, *rho* = 0.58), but not P content and growth rate ($p = 0.15$).

Figure S3. Addition and recovery of pure (a) DNA, (b) RNA, or (c) protein to cell lysate from *Roseovarius* sp. TM1035. Points represent the means ± sem from triplicate determinations. Detection values have been adjusted for the baseline signal from unamended cell lysate.

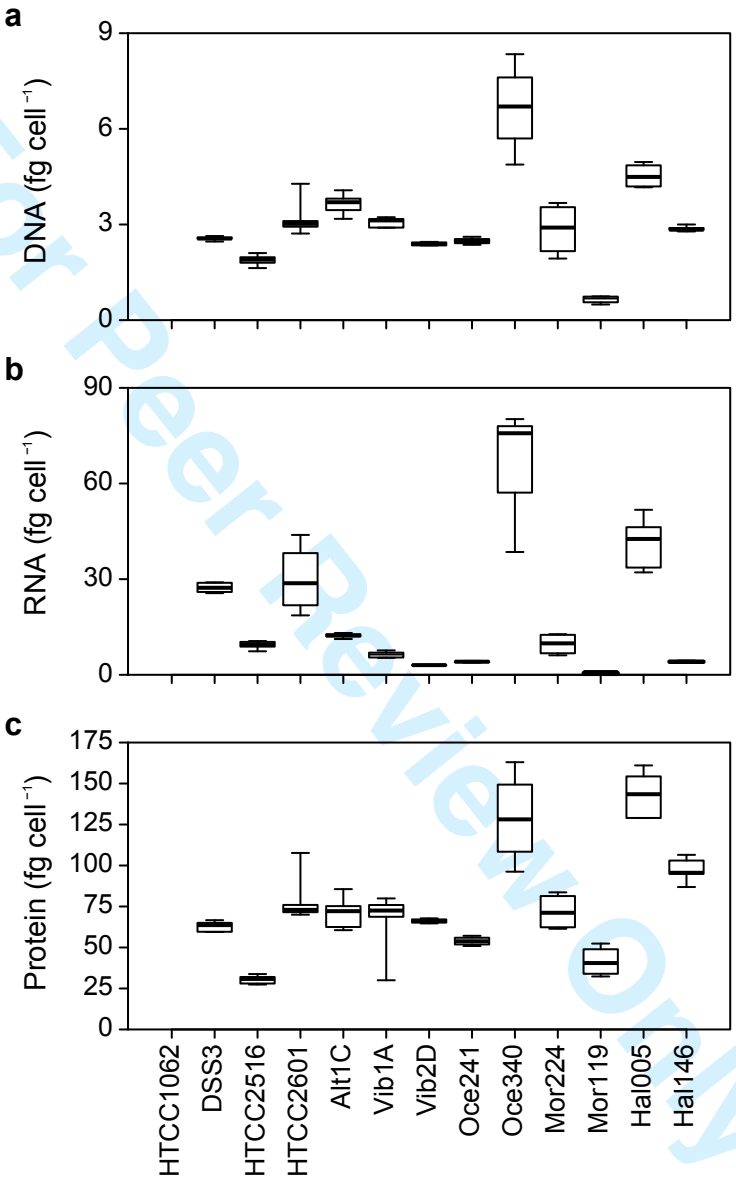

Figure S1

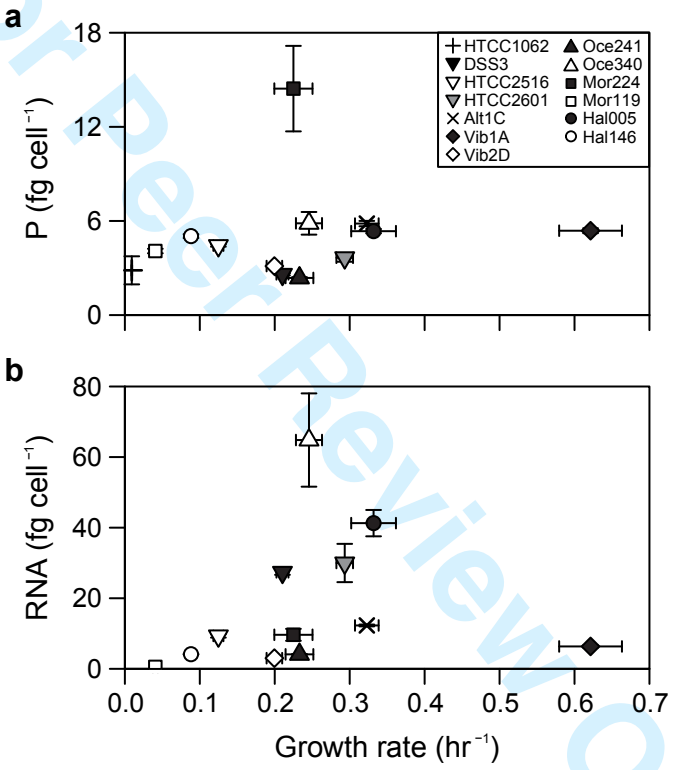

Figure S2

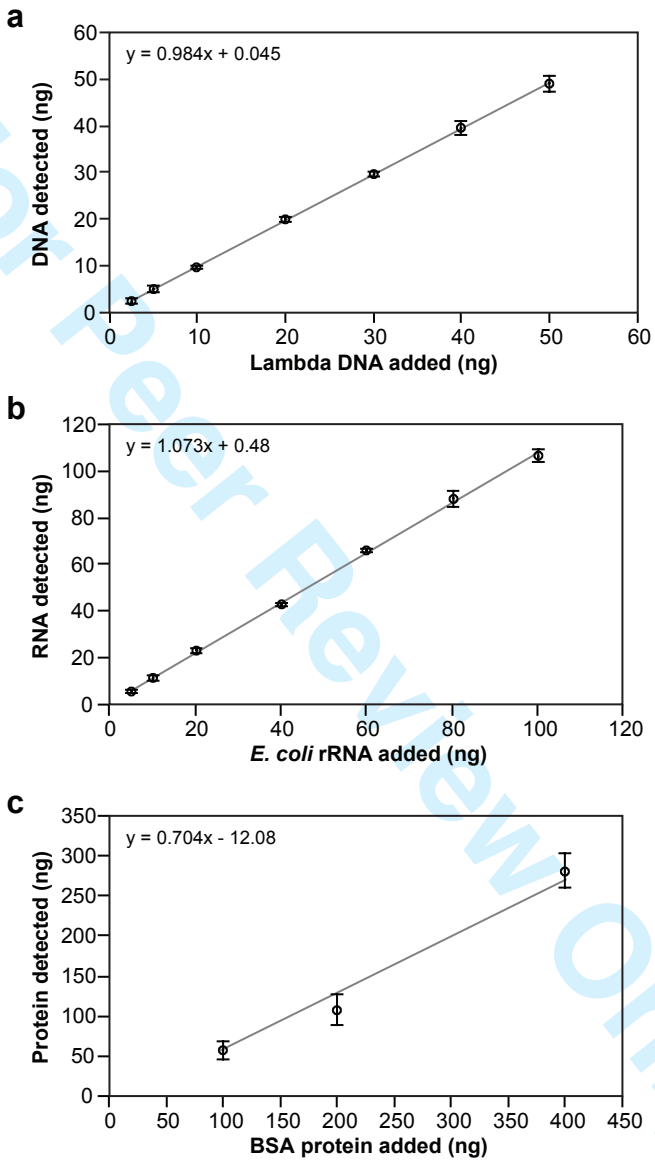

Figure S3